

## RESEARCH PAPER

# Identification of a novel snake peptide toxin displaying high affinity and antagonist behaviour for the $\alpha_2$ -adrenoceptors

Céline Rouget<sup>1</sup>, Loïc Quinton<sup>2</sup>, Arhamatoulaye Maïga<sup>1</sup>, Céline Gales<sup>3</sup>, Geoffrey Masuyer<sup>4</sup>, Christian Malosse<sup>5</sup>, Julia Chamot-Rooke<sup>5</sup>, Robert Thai<sup>1</sup>, Gilles Mourier<sup>1</sup>, Edwin de Pauw<sup>2</sup>, Nicolas Gilles<sup>1</sup> and Denis Servent<sup>1</sup>

<sup>1</sup>CEA, iBiTec-S, Service d'Ingénierie Moléculaire des Protéines (SIMOPRO), Gif sur Yvette, France, <sup>2</sup>Laboratoire de Spectrométrie de Masse, GIGA-R, University of Liège, Liège, Belgium, <sup>3</sup>INSERM U858, Department of Renal and Cardiac Remodeling, Toulouse, France, <sup>4</sup>Structural Molecular Biology Department of Biology & Biochemistry, University of Bath, Bath, UK, and <sup>5</sup>Laboratoire des Mécanismes Réactionnels, UMR 7651 CNRS, Ecole Polytechnique, Palaiseau, France

**Correspondence**

Dr Nicolas Gilles, CEA, Institute of Biology and Technologies (iBiTec-S), Service d'Ingénierie Moléculaire des Protéines (SIMOPRO), F-91191 Gif sur Yvette, France. E-mail: Nicolas.gilles@cea.fr

**Keywords**

three-finger-fold toxins; binding experiments;  $\alpha_2$ -adrenoceptor antagonists; venom fractionation; mass fragmentation; snake venoms

**Received**

19 February 2010

**Revised**

7 June 2010

**Accepted**

11 June 2010

**BACKGROUND AND PURPOSE**

Muscarinic and adrenergic G protein-coupled receptors (GPCRs) are the targets of rare peptide toxins isolated from snake or cone snail venoms. We used a screen to identify novel toxins from *Dendroaspis angusticeps* targeting aminergic GPCRs. These toxins may offer new candidates for the development of new tools and drugs.

**EXPERIMENTAL APPROACH**

In binding experiments with <sup>3</sup>H-rauwolscine, we studied the interactions of green mamba venom fractions with  $\alpha_2$ -adrenoceptors from rat brain synaptosomes. We isolated, sequenced and chemically synthesized a novel peptide,  $\rho$ -Da1b. This peptide was pharmacologically characterized using binding experiments and functional tests on human  $\alpha_2$ -adrenoceptors expressed in mammalian cells.

**KEY RESULTS**

$\rho$ -Da1b, a 66-amino acid peptide stabilized by four disulphide bridges, belongs to the three-finger-fold peptide family. Its synthetic homologue inhibited 80% of <sup>3</sup>H-rauwolscine binding to the three  $\alpha_2$ -adrenoceptor subtypes, with an affinity between 14 and 73 nM and Hill slopes close to unity. Functional experiments on  $\alpha_{2A}$ -adrenoceptor demonstrated that  $\rho$ -Da1b is an antagonist, shifting adrenaline activation curves to the right. Schild regression revealed slopes of 0.97 and 0.67 and pA<sub>2</sub> values of 5.93 and 5.32 for yohimbine and  $\rho$ -Da1b, respectively.

**CONCLUSIONS AND IMPLICATIONS**

$\rho$ -Da1b is the first toxin identified to specifically interact with  $\alpha_2$ -adrenoceptors, extending the list of class A GPCRs sensitive to toxins. Additionally, its affinity and atypical mode of interaction open up the possibility of its use as a new pharmacological tool, in the study of the physiological roles of  $\alpha_2$ -adrenoceptor subtypes.

**Abbreviations**

BRET, bioluminescence resonance energy transfer; EPA, 5-(N-ethyl-N-isopropyl)-amiloride; GPCR, G protein-coupled receptor; RBS, rat brain synaptosomes

## Introduction

Animal venoms represent a vast library of peptide toxins. With 1400 species of scorpions, 400 species of venomous snakes, 600 species of sea cone snails and 35 000 species of spiders, each with venoms containing more than 300 different toxins, this natural venom bank consists of more than 10 million peptide toxins, biochemically stable and with particular pharmacological properties. Currently, almost 1600 of these peptides have been sequenced (representing less than 0.02% of the natural bank), and this number is growing exponentially (King *et al.*, 2008). The ability to sequence toxins directly from mass spectrometry analysis of venoms, together with sequencing the genomes of venomous animals (Putnam *et al.*, 2007), will further accelerate the rate of peptide toxin discovery over the next few years. The pharmacological activity of toxins mainly arises from their action at ion channels, such as voltage-gated and ligand-gated ion channels, which are important in controlling the mobility of the venomous animal's prey (Terlau and Olivera, 2004). Thus, toxins targeting ion channels became valuable tools to study neurotransmission or neuromuscular junction and for labelling specific ion channels. Due to their high affinity and selectivity for various ion channels, some animal toxins are being used as drugs or are being tested in several preclinical trials (Becker and Terlau, 2008; Han *et al.*, 2008; Halai and Craik, 2009). For example, Prialt is a  $\omega$ -conotoxin, isolated from the venom of the cone snail species *Conus magus*, which selectively blocks N-type voltage-gated calcium channels and is the only approved non-opioid therapy for severe chronic pain (Williams *et al.*, 2008). Because venomous animals are predators that can quickly immobilize and kill their prey, it has been logical to consider only ion channels as the primary targets of toxins. Toxins are thus usually identified and characterized according to their toxicity (Terlau and Olivera, 2004). Consequently, very few alternative targets for toxins have been identified, and this includes the G protein-coupled receptors (GPCR) for which no extensive study has been performed. Of the 1600 known toxins, less than 30 are active at GPCRs and these can be divided into two families. Members of the first family mimic the natural agonist of the receptor target and include the snake sarafotoxins, functional analogs of the endogenous endothelins (Ducancel, 2005), the cone snail toxin conopressin, similar to the arginine-vasopressin peptide (Cruz *et al.*, 1987), or the cone snail toxin contulakin-G, similar to the neurotensin peptide (Craig *et al.*, 1999). The second family includes only 12 different toxins which are all

highly reticulated peptides with folds unrelated to natural ligands. Nine are active at muscarinic receptors and have been isolated from mamba venoms (Servent and Fruchart-Gaillard, 2009) and three are active at adrenergic receptors:  $\rho$ -TIA, from the conus *tulipa*, specific to the  $\alpha_{1B}$ -adrenoceptor (Sharpe *et al.*, 2001),  $\beta$ -cardiotoxin, from the snake *Ophiophagus Hannah*, active at  $\beta$ -adrenoceptors (Rajagopalan *et al.*, 2007) and  $\rho$ -Da1a (previously called AdTx1), from the snake *Dendroaspis angusticeps*, specific to the  $\alpha_{1A}$ -adrenoceptor (Quinton *et al.*, 2010). Due to their size and peptide nature, toxins acting on aminergic receptors display a range of atypical modes of action, including competitive and non-competitive interactions, insurmountable antagonism and negative allosterism. These toxins can be used to investigate the pharmacological and functional properties of their receptor targets and could also open new avenues for drug development (Harvey *et al.*, 2002; Chen *et al.*, 2004; Kukkonen *et al.*, 2004; Ducancel, 2005; Fruchart-Gaillard *et al.*, 2006; Antosova *et al.*, 2009). GPCRs are the molecular targets for almost half of currently used therapeutic drugs.

We have been studying green mamba venom to discover new toxins acting on aminergic GPCRs. Among the 300 different toxins detected by mass analysis in this venom (N. Gilles, unpubl. data), less than 10% are pharmacologically characterized. The first one, isolated more than 20 years ago (Adem *et al.*, 1988) and the last one identified 10 years later (Carsi *et al.*, 1999), interact with various subtypes of muscarinic acetylcholine receptors. We hypothesized that this venom contains more toxins active on GPCRs and recently discovered the first toxin specific for the  $\alpha_{1A}$ -adrenoceptor, which was initially called AdTx1 and then renamed according to a rational nomenclature  $\rho$ -Da1a (King *et al.*, 2008; Quinton *et al.*, 2010). Our strategy was based on the successive purification of venom associated with binding experiments using specific radiolabelled ligands and approximately 20 different receptors preparations. In this study, we described the identification of a novel peptide, called  $\rho$ -Da1b, which displays nanomolar affinities for the three  $\alpha_2$ -adrenoceptors subtypes and which antagonizes  $\alpha_{2A}$ -adrenoceptor activation non-competitively.

## Methods

### Venom fractionation

One gram of *Dendroaspis angusticeps* venom (Latoxan, Valence, France) was separated into 13 fractions by ion exchange (2 × 15 cm) on Source 15S using a protocol as previously described (Quinton

*et al.*, 2010). Fraction H was purified by reverse-phase chromatography (Waters 600, Milford, MA, USA) on a preparative column (C18, 15  $\mu\text{m}$ , 20 cm, Vydac, Sigma-Aldrich, Saint Quentin Fallavier, France, 10 mL $\cdot\text{min}^{-1}$ ), using a linear gradient from 0 to 100% acetonitrile and 0.1% trifluoroacetic acid in 100 min. Fraction D was further purified on an analytical HPLC C18 Vydac column (4.6 mm, 5  $\mu\text{m}$ , 15 cm 1 mL $\cdot\text{min}^{-1}$ ) using a gradient of 0.5% acetonitrile $\cdot\text{min}^{-1}$ .

### Protein quantification

Fraction A protein concentration and membrane protein concentration were determined using the Bio-Rad (Hercules, CA, USA) protein assay, with bovine serum albumin (BSA) as standard.

### Edman sequencing

N-terminal sequencing of fraction A (100 pmol loaded on a Biobrene-coated filter) was carried out using Edman chemistry on a Procise Model 492 automatic sequencer from Applied Biosystems (Foster City, CA, USA).

### Mass spectrometry analysis

Mass spectrometry was carried out with a 7-T APEX III FT-ICR mass spectrometer (Bruker Daltonics, Bremen, Germany) equipped with a 7 Tesla magnet. A voltage of  $-700\text{ V}$  was applied between the nano-electrospray needles (Proxeon, Odense, Denmark) and the entrance of the glass capillary, for ion transfer at a temperature of  $50^\circ\text{C}$ . Mass spectra were acquired from  $m/z$  200 to 3000 with 512 k data points. Monoisotopic peaks were labelled using XMASS 6.1.4 software (Bruker Daltonics). Peptides were sequenced by MALDI-'in-source decay', peptide mass fingerprinting and MS/MS experiments on an ULTRAFLEX II MALDI-TOF/TOF (Bruker Daltonics) mass spectrometer equipped with a Nd-YAG Smartbeam laser (MLN 202, LTB). 1,5-Diaminonaphthalene saturated in acetonitrile/formic acid 0.1% 50/50 (v/v) was used for in-source decay and 2,5-dihydroxybenzoic acid at 20 mg $\cdot\text{mL}^{-1}$  in acetonitrile/formic acid 0.1% 50/50 (v/v) was used for peptide mass fingerprinting and MS/MS experiments.  $\rho$ -Da1b (about 70 ng) was reduced by 5  $\mu\text{L}$  of 100 mM dithiothreitol in 100 mM  $\text{NH}_4\text{HCO}_3$  for 1 h at  $50^\circ\text{C}$  and then alkylated by 1  $\mu\text{L}$  of 500 mM iodoacetamide for 45 min in the dark before hydrolysis with 1 ng of trypsin (sequencing grade, from bovine pancreas), overnight at  $37^\circ\text{C}$ . The resulting peptides were desalted using a Zip-Tip C18 microcolumn (Millipore, Billerica, MA, USA), spotted on the DHB matrix and analyzed by MALDI-TOF/TOF.

### Synthesis of $\rho$ -Da1b

$\rho$ -Da1b was synthesized on an Applied Biosystems 433A peptide synthesizer, purified and folded according to the method described for the muscarinic toxin MT1 (Mourier *et al.*, 2003). Briefly, this involved solid-phase synthesis using a Fmoc strategy, peptide cleavage and purification on a reverse-phase column. The linear peptide was then folded at  $4^\circ\text{C}$  for 48 h in the presence of glycerol (25%) and oxidized and reduced glutathione (1 mM) in Tris buffer at pH 8.

### Animals

All animal care and experimental procedures were in compliance with French legislation, following the European Council Directive 86/609/EEC regarding the protection of animals used for experimental purposes.

### Toxins and molecular targets nomenclature

Receptor nomenclature follows Alexander *et al.* (2009). Toxin nomenclature follows the recent suggestions from the International Society on Toxinology (Tytgat *et al.*, 1999; King *et al.*, 2008).

### Binding analysis

Rat brain synaptosomes (RBS) were prepared from adult albino Sprague Dawley rats (Favreau *et al.*, 2001). After dissection, the entire brain was homogenized in ice-cold 0.3 M mannitol buffer containing 10 mM EDTA and 10 mM HEPES-Tris, pH 7.4. After centrifugation at  $1000\times g$  for 10 min, the supernatant was removed and centrifuged at  $27\,000\times g$  for 30 min (P2 pellet). All buffers contained a cocktail of protease inhibitors composed of: phenylmethylsulphonyl fluoride (50 mg $\cdot\text{mL}^{-1}$ ), pepstatin A (1 mM), iodoacetamide (1 mM) and 1 mM f 1,10-phenanthroline. Human  $\alpha_2$ -adrenoceptors and  $\alpha_1$ -adrenoceptors subtypes were stably expressed in mammalian CHO cells kindly provided by Dr Paris, INSERM 858, Toulouse, France and Dr Cottechia, Lausanne University, Switzerland, respectively. Membranes from CHO cells were prepared as described previously (Fruchart-Gaillard *et al.*, 2006). Membranes from cells expressing  $\beta$ -adrenoceptors were purchased from PerkinElmer (Courtaboeuf, France). Binding experiments were performed in 96-well plates. Reaction mixtures contained 50 mM Tris-HCl, pH 7.4, 10 mM  $\text{MgCl}_2$  and 1 g $\cdot\text{L}^{-1}$  BSA in a final volume of 100  $\mu\text{L}$ . Plates were incubated for 16 h (except for the kinetic experiments) at room temperature. Binding reactions were stopped by filtration through a GF/C filter pre-soaked in 0.5% polyethyleneimine on a cell harvester (PerkinElmer) and plates were dried. Ultimagold O (25  $\mu\text{L}$ ;

PerkinElmer) was added to each well and samples were counted using a TopCount counter (PerkinElmer) (Counting yield of 55%). Non-specific binding was measured in the presence of 1  $\mu\text{M}$  prazosin for  $^3\text{H}$ -prazosin binding, 1  $\mu\text{M}$  yohimbine for  $^3\text{H}$ -rauwolscine, 3  $\mu\text{M}$  propranolol for  $^3\text{H}$ -CGP-12177 and was subtracted from the total binding. A one-site inhibition mass action curve was fitted to inhibition binding data using Kaleidagraph (Synergy software, Reading, PA, USA).  $\text{IC}_{50}$  values were converted to  $K_i$  for competition experiments using the Cheng-Prusoff equation (Cheng and Prusoff, 1973). Equilibrium saturation experiments were performed with various concentrations of radioactive ligand and a constant quantity of membrane. Kinetic experiments were carried out using a constant amount of radioactive ligand and membrane, with various incubation times. The dissociation kinetics of  $^3\text{H}$ -rauwolscine were determined after addition of 1  $\mu\text{M}$  of rauwolscine and 10  $\mu\text{M}$  of  $\rho$ -Da1b. The dissociation rate constant ( $k_{\text{off}}$ ) was determined directly from a first-order plot of ligand dissociation versus time. Binding results are presented as mean  $\pm$  SD (standard deviation) with  $n$ , number of independent experiments.

### *Bioluminescence resonance energy transfer measurement*

We used bioluminescence resonance energy transfer (BRET) to follow the structural changes of the G trimeric protein under receptor activation, as previously described (Gales *et al.*, 2006). BRET signals were measured in HEK293T cells coexpressing  $\text{G}\alpha_{i1}$ -Renilla luciferase (RLuc) (RLuc energy donor inserted at position 91 of amino acid sequence of  $\text{G}\beta_{11}$ ), GFP10-G $\gamma$ 2 (GFP10 energy acceptor inserted at the N-terminus of G $\gamma$ 2) and in the presence of the complementary  $\text{G}\beta_1$  subunits and  $\alpha_{2A}$ -adrenoceptor. Measurements were conducted in resuspended cells in 96-well microplates (white optiplate; PerkinElmer). BRET readings were collected 1 min after addition of 5  $\mu\text{M}$  coelenterazine 400a (Optima), using Infinite F500 (Tecan group Ltd, Männedorf, Switzerland) that allows sequential integration of signals emitted by GFP10 and RLuc. Results are expressed as the difference in BRET signals measured between the BRET partners in the presence and absence of the  $\alpha_{2A}$ -adrenoceptor-agonist UK14304 (10  $\mu\text{M}$ , UK-modulated BRET). Results are expressed as mean  $\pm$  SD with  $n$ , number of independent experiments.

### *Functional tests on human- $\alpha_{2A}$ -adrenoceptor*

Functional tests were carried out in 96-well plates using COS cells transfected with DNA encoding the human  $\alpha_{2A}$ -adrenoceptor (33 ng/well) and the ubiqui-

itous G protein GqTop [16.6 ng/well, kindly provided by Dr J.P. Pin, Montpellier, France (Selvam *et al.*, 2010)], using the lipofectamine reagent (according to the manufacture protocol). Forty-eight hours after transfection, cells were incubated for 1 h at 37°C with 10  $\mu\text{L}$  of 10 $\times$  solutions of the various compounds tested and 100  $\mu\text{L}$  of dye solution (FLIPR Calcium Kit buffer, Molecular Devices, Sunnyvale, CA, USA) supplemented with 2.5 mM probenecid. Changes in fluorescence induced by adrenaline were measured at 37°C using a Flex station I (Molecular Devices), with an excitation wavelength of 485 nm and emission wavelength of 525 nm. The resulting activation curves obtained were analyzed using Softmax Pro software (Molecular Devices). Receptor activation for the different experimental conditions was evaluated using maximum and minimum values and analyzed by Kaleidagraph (Synergy software). Results are expressed as mean  $\pm$  SD with  $n$ , number of independent experiments.

### *Materials*

Radioactive components were from PerkinElmer. All chemical products and cell culture media were from Sigma-Aldrich. Protected amino acid derivatives and resins were from Novabiochem (France Biochem, Meudon, France).

## **Results**

### *Isolation and characterization of $\rho$ -Da1b*

Green mamba venom was separated into 13 fractions by cation exchange chromatography (Figure 1A). We investigated the capacity of each fraction to inhibit  $^3\text{H}$ -rauwolscine binding to RBS. Fraction H, which significantly reduced  $^3\text{H}$ -rauwolscine binding, was sub-fractionated by reverse-phase chromatography (Figure 1B). Pharmacological activity was recovered in peak D. This fraction, composed of one major (average mass of 6826 Da) and one minor (average mass of 7512 Da) toxin, was further fractionated by reverse phase chromatography (Figure 1C). The minor fraction A, determined to be around 200  $\mu\text{M}$  concentration, inhibited  $^3\text{H}$ -rauwolscine binding in a concentration-dependent manner, giving a binding curve with a Hill slope of around 0.75 and with an affinity in the nanomolar range (Figure 1D). The monoisotopic molecular mass of the toxin was, after deconvolution of 7507.507 Da (Figure 2A) and 7515.582 Da, before and after reduction, respectively, indicating the presence of four disulphide bonds. Its sequence was determined by a combination of Edman's degradation (for the 54 first residues) and mass analysis. After reduction, the toxin was fragmented by In-source Decay (Quinton *et al.*,



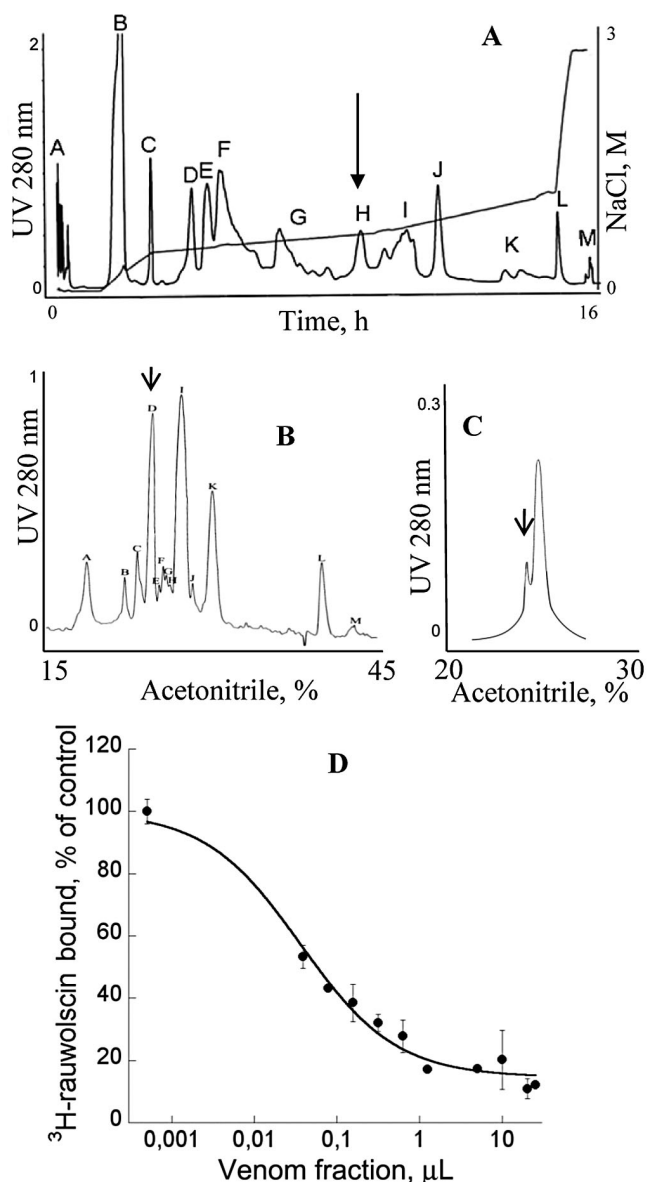


**Figure 1**

Purification and preliminary pharmacological characterization of  $\rho$ -Da1b. (A) Ion-exchange chromatography of *Dendroaspis angusticeps* crude venom. Labeled peaks were collected (13 fractions). (B) Reverse-phase chromatography of fraction H on a Vydac C18 preparative column. Labeled peaks were collected (20 fractions). Fraction D was eluted at around 27% acetonitrile. (C) Reverse-phase chromatography of fraction D on a Vydac C18 analytical column. Arrows show active peaks. (D) Inhibition of  $^3\text{H}$ -rauwolscine (1 nM) binding on rat brain synaptosomes by the minor peak purified in C.

2007). A *c*-ion series was generated, allowing characterization of 48 central amino acids out of a total of 66 (73% sequence coverage, results not shown), but leaving the N- and C-terminal ends undetermined. To determine the C-terminal part of the toxin sequence,  $\rho$ -Da1b was hydrolyzed by trypsin and the peptide mixtures were analyzed by MALDI-TOF/TOF (Figure 2B). The ion at  $m/z$  1680.68, corresponding to

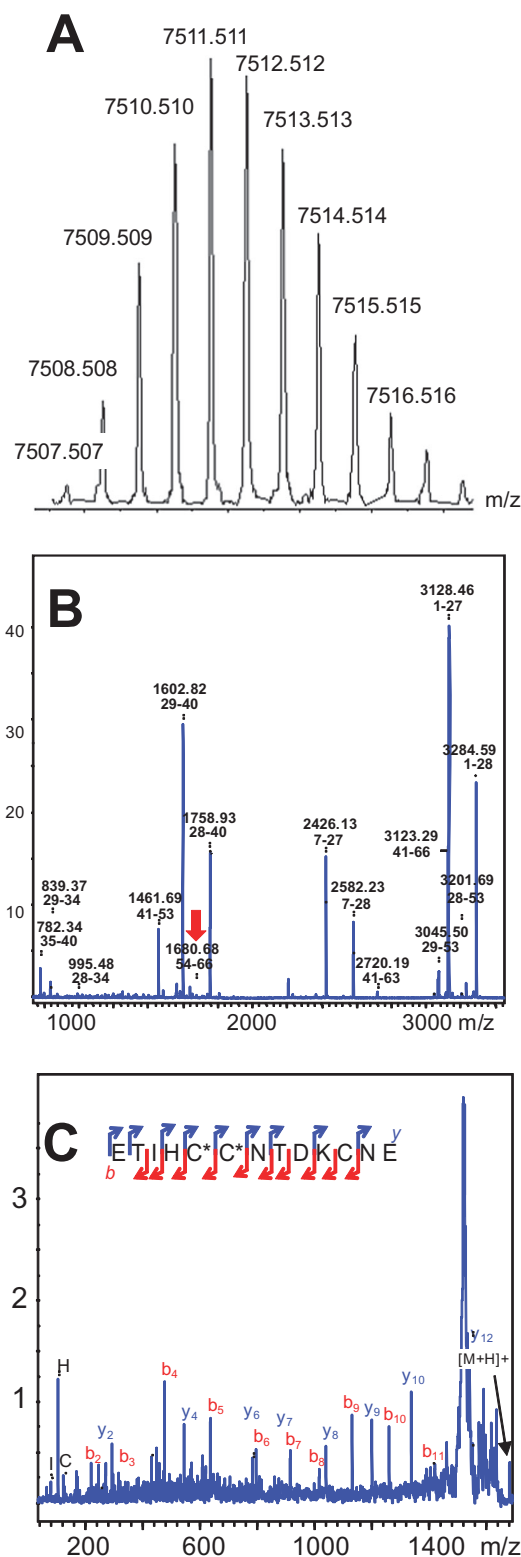


**Figure 2**

Mass and sequence analysis of  $\rho$ -Da1b. (A) Isotopic profile of  $\rho$ -Da1b. (B) Peptide mass fingerprint of  $\rho$ -Da1b after trypsin treatment. (C) Fragmentation by MALDI-LIFT-TOF/TOF of the  $m/z$  1680.68 ion (red arrow) obtained after trypsin digestion. *b*- and *y*-ion types used for the sequencing are indicated in red and blue, respectively.

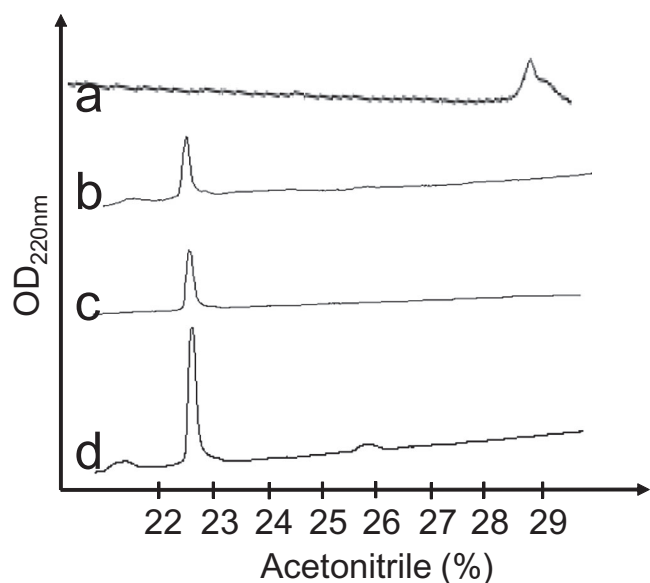


**Figure 3**

Analytical reverse-phase chromatography of the reduced synthetic  $\rho$ -Da1b (line a), oxidized synthetic  $\rho$ -Da1b (line b) and natural  $\rho$ -Da1b (line c). Line d shows the co-elution of the natural and synthetic oxidized  $\rho$ -Da1b.

the C-terminus part (red arrow), was selected and fragmented by LIFT-TOF/TOF (Suckau *et al.*, 2003). The fragmentation spectrum (Figure 2C) revealed  $y$  and  $b$ -ion fragments, allowing the C-terminus sequence to be determined without any ambiguity since the accuracy of mass measurement is less than 0.5  $m/z$ . Determination of the whole sequence thus gave LTCVTKDTIFGITTQNCAPGQNLFCFIRRHYYINHRYTEITRGCTATCPKPTNVRETIHCCNTDKCNE. This sequence has a theoretical mass (7507.4869 Da) differing by 2.7 ppm from the experimental value. We chemically synthesized, purified and refolded the corresponding peptide, as previously described (Mourier *et al.*, 2003). Comparative analytical HPLC showed that the synthetic linear-reduced peptide (Figure 3, line a) was more hydrophobic than the folded and oxidized form (Figure 3, line b), which was eluted at the same position as the native peptide (Figure 3, line c), as confirmed by co-injection of both peptides (Figure 3, line d). We named this new peptide  $\rho$ -Da1b. The Greek letter signifies its activity at adrenoceptors, Da corresponds to the animal genus (*Dendroaspis angusticeps*), 1 relates to the three-finger fold of the peptide and b to the second homologue toxin, the first one being  $\rho$ -Da1a, specific to the  $\alpha_{1A}$ -adrenoceptor, previously called AdTx1 (McIntosh *et al.*, 1999; Tytgat *et al.*, 1999; King *et al.*, 2008; Quinton *et al.*, 2010). Protein sequence data reported here have been deposited in the UniProt database under accession number P86419.

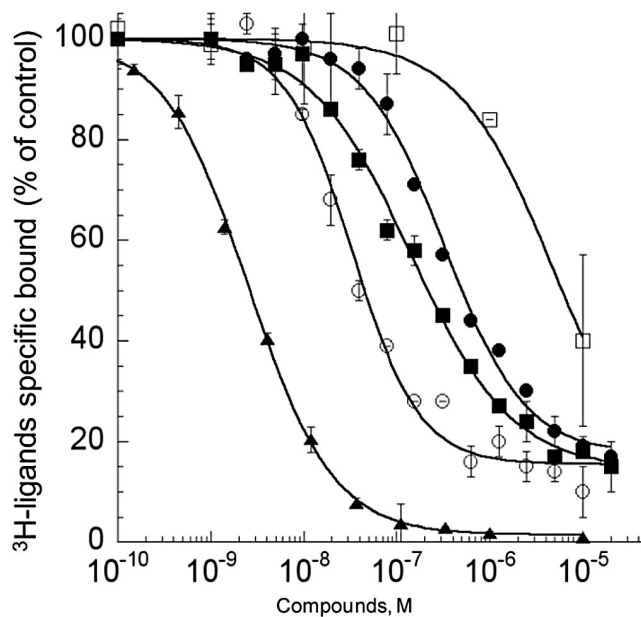


**Figure 4**

Inhibition binding curves for human adrenoceptors of  $^3\text{H}$ -rauwolscine (1 nM) in CHO membranes expressing,  $\alpha_{2A}$ -adrenoceptor (12  $\mu\text{g}$ ) with yohimbine ( $\blacktriangle$ ) and  $\rho$ -Da1b ( $\circ$ ) and membranes expressing  $\alpha_{2B}$  (11  $\mu\text{g}$ ,  $\blacksquare$ ) or  $\alpha_{2C}$ -adrenoceptor (3.1  $\mu\text{g}$ ,  $\bullet$ ) with  $\rho$ -Da1b. Inhibition of  $^3\text{H}$ -prazosin (1 nM) by  $\rho$ -Da1b in CHO membranes expressing  $\alpha_{1A}$ -adrenoceptor (3.8  $\mu\text{g}$ ).

#### *$\rho$ -Da1b is specific for $\alpha_2$ -adrenoceptors*

We first characterized the binding of  $^3\text{H}$ -rauwolscine to the three  $\alpha_2$ -adrenoceptor subtypes stably expressed in CHO cells. Saturation binding experiments performed with increasing concentrations of  $^3\text{H}$ -rauwolscine (0.1 to 7 nM) were used to obtain affinities of the tritiated ligand and the number of ligand-binding sites present on the cells expressing the receptor.  $^3\text{H}$ -rauwolscine had an affinity of 0.83 nM, with a  $B_{\text{max}}$  (in pmol/mg membrane protein) of 1.6 pmol $\cdot$ mg $^{-1}$ , for the  $\alpha_{2A}$ -adrenoceptor; an affinity of 0.97 nM and  $B_{\text{max}}$  of 2.1 pmol $\cdot$ mg $^{-1}$  for the  $\alpha_{2B}$  subtype; and an affinity of 0.15 nM with a  $B_{\text{max}}$  of 27 pmol $\cdot$ mg $^{-1}$  for  $\alpha_{2C}$ -adrenoceptors (data not shown). These rauwolscine  $K_d$  values were used to calculate  $K_i$  values for  $\rho$ -Da1b using the Cheng-Prusoff equation.  $\rho$ -Da1b inhibited  $^3\text{H}$ -rauwolscine binding with an  $\text{IC}_{50}$  of  $28.1 \pm 4.1$  nM, a  $K_i$  value of  $14 \pm 2$  nM and a Hill slope of 1.2 for  $\alpha_{2A}$ -adrenoceptors; an  $\text{IC}_{50}$  of  $144 \pm 12$  nM, a  $K_i$  value of  $73 \pm 6$  nM and a Hill slope of 0.80 for  $\alpha_{2B}$ -adrenoceptors; and an  $\text{IC}_{50}$  of  $260 \pm 40$  nM, a  $K_i$  value of  $38 \pm 6$  nM and a Hill slope of 1.0 for  $\alpha_{2C}$ -adrenoceptors ( $n = 3$ , Figure 4). To confirm the selectivity of  $\rho$ -Da1b for adrenoceptor type, we evaluated its inhibition of  $^3\text{H}$ -prazosin binding to the three  $\alpha_1$ -adrenoceptor subtypes and  $^3\text{H}$ -CGP12177 binding to the three  $\beta$ -adrenoceptors.

The toxin inhibited  $^3\text{H}$ -prazosin binding to the h- $\alpha_{1A}$ -adrenoceptor with an  $\text{IC}_{50}$  of  $6.4 \pm 2.2 \mu\text{M}$ , corresponding to a  $K_i$  of  $2.1 \pm 0.7 \mu\text{M}$  and a Hill slope of 0.84 ( $n = 2$ , Figure 4) but did not affect binding, at a concentration of  $10 \mu\text{M}$ , for any of the other subtypes tested (data not shown).

Regardless of the  $\alpha_2$ -adrenoceptor subtype used,  $\rho$ -Da1b could not totally abolish  $^3\text{H}$ -rauwolscine binding, leaving residual binding between 15 and 20%. This contrasts with yohimbine, which is able to fully displace  $^3\text{H}$ -rauwolscine binding, with a  $K_i$  of  $0.85 \pm 0.01 \text{ nM}$  and a Hill slope of 0.96 (Figure 4).

### *$\rho$ -Da1b prevents $\alpha_{2A}$ -adrenoceptor-induced activation of $G_i$*

Activation of GPCR induces conformational changes in the associated trimeric G protein. This structural reorganization can be studied using a system in which  $G\alpha_i$  is fused to the RLuc ( $G\alpha_{i1}$ -RLuc) and  $G\gamma_2$  is fused to the fluorescent protein GFP ( $GFP_{10}$ - $G\gamma_2$ , Figure 5A). Addition of coelenterazine induces emission of light by RLuc, which leads to the activation of GFP if the two protein constructs are in close proximity, that is, in this case, if the constituents of the trimeric G protein remain associated (Figure 5A). We tested the capacity of yohimbine and  $\rho$ -Da1b to activate or antagonize the  $\alpha_{2A}$ -adrenoceptor. Receptor activation was not observed upon addition of  $10 \mu\text{M}$  of yohimbine or  $\rho$ -Da1b (Figure 5B), whereas  $10 \mu\text{M}$  UK14304 significantly reduced the BRET signal, consistent with its action as a specific  $\alpha_2$ -adrenoceptor agonist. Cells were then pretreated for 1 h with  $10 \mu\text{M}$  yohimbine or  $\rho$ -Da1b and then stimulated with UK14304. Both yohimbine and  $\rho$ -Da1b significantly reduced the agonist-induced activation of the  $\alpha_{2A}$ -adrenoceptor, demonstrating their antagonist activity at this receptor ( $n = 3$ , Figure 5B).

### *Characterization of the $\rho$ -Da1b antagonist potency on $\alpha_{2A}$ -adrenoceptors*

The  $\rho$ -Da1b antagonist properties were further evaluated in functional experiments on COS mammalian cells co-expressing the h $\alpha_{2A}$ -adrenoceptor and the chimeric G protein GqTop (Selvam *et al.*, 2010), allowing the cell signal response to be measured by calcium release. Receptor activation was followed with a fluorophore sensitive to the intracellular  $\text{Ca}^{2+}$  concentration. Cells were pre-incubated with antagonists (from 0 to  $100 \mu\text{M}$ ) for 2 h before addition of adrenaline (1 nM to  $300 \mu\text{M}$ ). The  $\text{EC}_{50}$  of adrenaline without pre-incubation with antagonist was  $0.16 \pm 0.03 \mu\text{M}$  ( $n = 8$ ). Activation curves shifted to the right with increased antagonist concentration, without changing adrenaline efficacy. The shifts were significantly greater in the presence

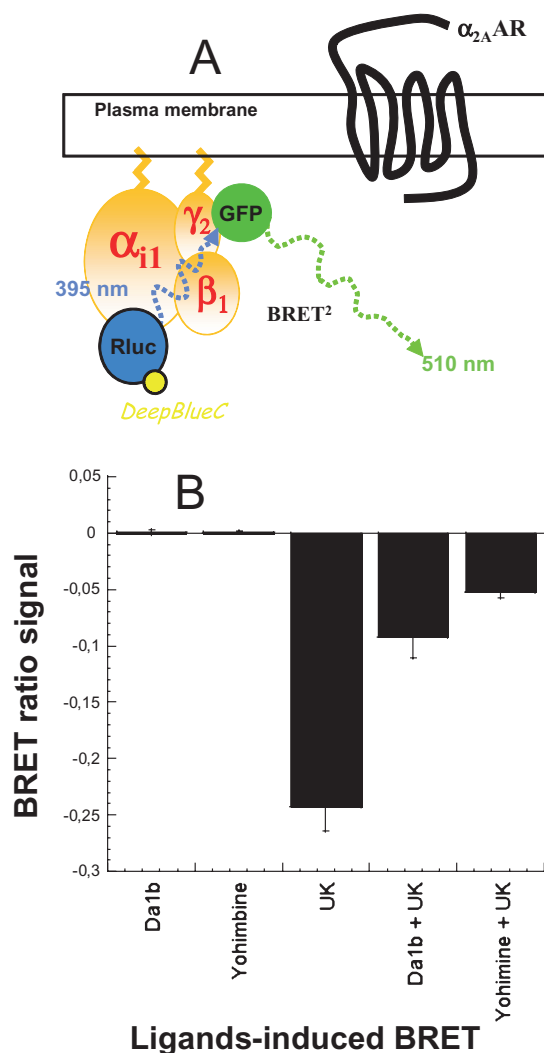


**Figure 5**

$\rho$ -Da1b prevented  $\alpha_{2A}$ -adrenoceptor mediated  $G_i$ -inhibition. (A) Construction of the trimeric G protein with Renilla luciferase (RLuc) as a donor and GFP as acceptor link to the  $\alpha_{i1}$  and  $\gamma_2$  subunits, respectively. (B) Cells were first treated directly with  $10 \mu\text{M}$   $\rho$ -Da1b or yohimbine to evaluate their agonistic property. Results are expressed as the difference in bioluminescence resonance energy transfer (BRET) signals measured before and after application of the compounds. Then, cells were stimulated with  $10 \mu\text{M}$  UK14304 alone or after a pre-incubation with  $10 \mu\text{M}$  of  $\rho$ -Da1b or yohimbine. Results are expressed as the difference in BRET signals measured before and after the  $\alpha_2$ -agonist UK14304 stimulation. Data represent the mean  $\pm$  SD of three independent experiments.

of yohimbine ( $\text{EC}_{50}$  between  $0.16$  and  $12.0 \mu\text{M}$ , Figure 6A) than in the presence of  $\rho$ -Da1b ( $\text{EC}_{50}$  between  $0.16$  and  $2.21 \mu\text{M}$ , Figure 6B). Hill slopes of the activation curves remained close to 1 for yohimbine and  $\rho$ -Da1b (Table 1). Schild regressions (Figure 6C) were linear for both antagonists, with a slope close of 0.97 for yohimbine and 0.67 for  $\rho$ -Da1b. The  $\text{pA}_2$  values calculated were 5.93 for yohimbine and 5.32 for  $\rho$ -Da1b.

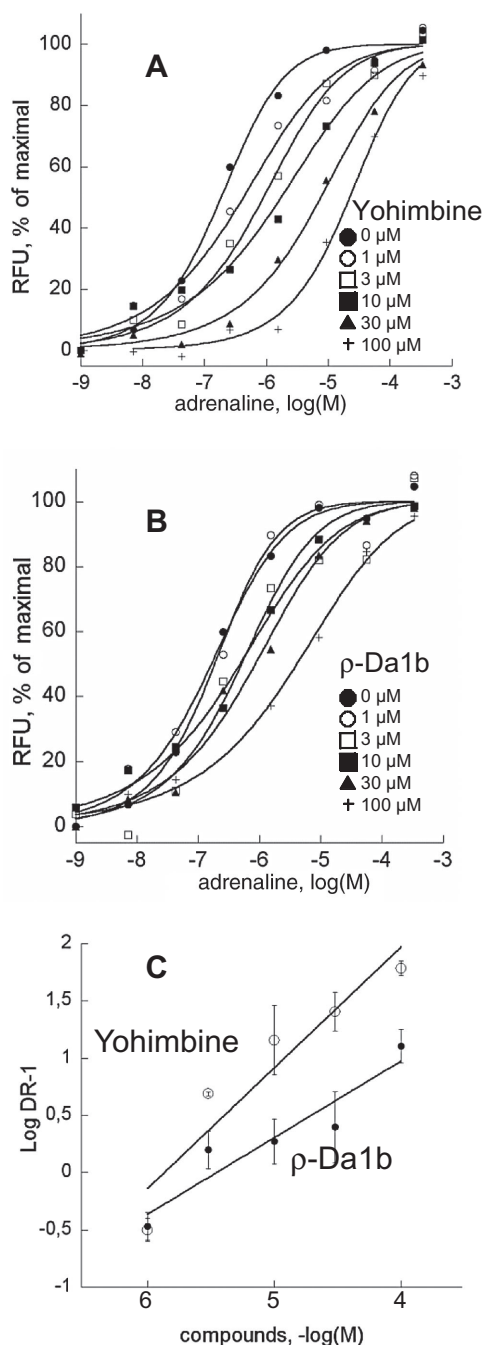


**Figure 6**

Functional characterization of yohimbine and  $\rho$ -Da1b on COS cells co-expressing the  $\alpha_{2A}$ -adrenoceptor and the chimeric G protein GqTop. Concentration–response curves for epinephrine were obtained in the presence of increasing concentrations of yohimbine (A) or  $\rho$ -Da1b (B). Error bars have been omitted for clarity. (C) Schild plot representations of the evolution of epinephrine  $EC_{50}$  in the presence of yohimbine (○) or  $\rho$ -Da1b (●) were fitted by a linear regression.

### Characterization of the mode of action of $\rho$ -Da1b on $\alpha_{2A}$ -adrenoceptors

As described above,  $\rho$ -Da1b, in contrast to yohimbine, could not fully inhibit  $^3H$ -rauwolscine binding

to  $\alpha_2$ -adrenoceptors and antagonized activation by adrenaline, with a non-competitive mechanism. To further characterize the mode of interaction of  $\rho$ -Da1b with  $\alpha_{2A}$ -adrenoceptor, we performed additional equilibrium and kinetic binding experiments.

Saturation binding experiments were carried out with COS cells transiently expressing the human  $\alpha_{2A}$ -adrenoceptor. We first checked that, using this expression system,  $\rho$ -Da1b inhibits  $^3H$ -rauwolscine with the same affinity and induces the same amount of residual binding as observed for stable CHO cell lines (data not shown). Saturation binding experiments with  $^3H$ -rauwolscine gave an affinity of  $2.5 \pm 0.2$  nM with a membrane capacity of  $27 \pm 1$  pmol of receptor (mg protein) $^{-1}$ . With a large excess of  $\rho$ -Da1b (10  $\mu$ M),  $^3H$ -rauwolscine affinity was  $4.0 \pm 1.1$  nM, with a membrane capacity of  $7.0 \pm 0.5$  pmol of receptor (mg protein) $^{-1}$  (Figure 7A). Thus, the presence of  $\rho$ -Da1b did not significantly modify  $^3H$ -rauwolscine affinity constant but reduced the number of accessible ligand binding sites at the membrane by a factor of four.

Most allosteric modulators affect the orthosteric ligand dissociation rate. We measured the  $K_{off}$  for  $^3H$ -rauwolscine (Figure 7B) in the presence of 1  $\mu$ M of rauwolscine alone ( $K_{off \text{ rauwolscine}} = 0.024 \pm 0.005$  min $^{-1}$ ,  $n = 4$ ) and in the presence of rauwolscine with  $\rho$ -Da1b (10  $\mu$ M) ( $K_{off \text{ rauwolscine}+\rho\text{-Da1b}} = 0.029 \pm 0.008$  min $^{-1}$ ,  $n = 3$ ) or with 1 mM of 5-N-ethyl-N-isopropyl-amiloride (EPA,  $K_{off \text{ rauwolscine}+\text{EPA}} = 0.058 \pm 0.004$  min $^{-1}$ ,  $n = 3$ ). Whereas the rauwolscine dissociation rate was doubled in the presence of EPA, consistent with previous observations (Leppik *et al.*, 2000), it was not significantly affected by  $\rho$ -Da1b. Finally, we measured the  $^3H$ -rauwolscine dissociation rate in the presence of 10  $\mu$ M of  $\rho$ -Da1b alone. The kinetic rate obtained under these conditions ( $K_{off \rho\text{-Da1b}} = 0.021 \pm 0.007$  min $^{-1}$ ,  $n = 3$ ) was similar to that obtained for rauwolscine alone, suggesting a competitive mechanism of action for the toxin. Additionally, only 80% of  $^3H$ -rauwolscine binding was reversed by  $\rho$ -Da1b, consistent with equilibrium binding experiments.

## Discussion

Screening green mamba venom against GPCR targets enabled us to isolate  $\rho$ -Da1b, the second original toxin active on adrenoceptors. Analysis of the  $\rho$ -Da1b sequence demonstrated that this toxin belongs to the three-finger-fold toxin family, one of the most common folds found in snake venoms. This fold consists of 61 to 74 residues, reticulated by four conserved disulphide bridges. The tips of the fingers usually constitute the active site, with the



**Table 1**

Maximal signal (Max, arbitrary units), EC<sub>50</sub> ( $\mu$ M) and Hill slope ( $n_H$ ), for activation by adrenaline in the presence of various concentrations of yohimbine and  $\rho$ -Da1b

		Antagonists					
		0 $\mu$ M	1 $\mu$ M	3 $\mu$ M	10 $\mu$ M	30 $\mu$ M	100 $\mu$ M
Yohimbine	EC <sub>50</sub>	0,16 $\pm$ 0,03	0,508 $\pm$ 0,087	0,681 $\pm$ 0,37	1,61 $\pm$ 1,2	4,11 $\pm$ 1,1	12,0 $\pm$ 5,8
	$n_H$	1.11	0.93	0.96	0.87	0.89	0.96
	Max	6060 $\pm$ 1010	4306 $\pm$ 585	6536 $\pm$ 150	6299 $\pm$ 776	5151 $\pm$ 165	5787 $\pm$ 660
	$n$	8	3	3	6	4	6
$\rho$ -Da1b	EC <sub>50</sub>	0.16 $\pm$ 0.03	0.173 $\pm$ 0.038	0.419 $\pm$ 0.098	0.611 $\pm$ 0.48	0.745 $\pm$ 0.56	2.21 $\pm$ 0.68
	$n_H$	1.11	1.04	1.01	0.89	0.92	0.81
	Max	6060 $\pm$ 1010	6766 $\pm$ 186	6125 $\pm$ 762	6414 $\pm$ 701	6680 $\pm$ 1243	7232 $\pm$ 126
	$n$	8	3	4	6	6	3

$n$ , number of experiments.

palm of the 'hand' formed by the four bridges. Some three-finger-fold toxins have an additional disulphide bridge located at the tip of the first or second finger, affecting their pharmacological profiles (Agrawal *et al.*, 1984; Servent *et al.*, 1997). The three-finger-fold toxin was initially described for its activity at nicotinic acetylcholine receptors (Changeux *et al.*, 1970). Since this finding, many other pharmacological activities have been attributed to this toxin family. Most three-finger-fold toxins interact with cholinergic systems, including nicotinic receptors, muscarinic acetylcholine receptors and acetylcholinesterases (Servent and Menez, 2001). However, toxins from this family also interact with coagulation factors (Banerjee *et al.*, 2005), calcium channels (de Weille *et al.*, 1991), phospholipids (Kumar *et al.*, 1997) and integrin receptors (Wu *et al.*, 2006). Recent findings have described two new three-finger-fold toxins, one is active on  $\beta$ -adrenoceptors (Rajagopalan *et al.*, 2007) and the other on  $\alpha_{1A}$ -adrenoceptors (Quinton *et al.*, 2010). Indeed, the three-finger-fold toxin family is probably associated with the most diverse range of characterized pharmacological activities for toxins to date.

In this study, the four peptides sharing the highest level of sequence identity (74–77%) with  $\rho$ -Da1b were MT $\alpha$ , from *Dendroaspis polylepis*, and MT3, MT4 and MT1 from *Dendroaspis angusticeps* (Table 2). These toxins are all active at muscarinic receptors (Joubert, 1985; Jolkkonen *et al.*, 1995, 2001), although MT1 also binds to  $\alpha_1$ -adrenoceptors (Harvey *et al.*, 2002). The second most similar group of toxins, showing 64 to 67% identity with  $\rho$ -Da1b, included  $\rho$ -Da1a, MT $\beta$  and Cm3. Nothing is known about the pharmacological characteristics of Cm-3, except that it is not toxic at the high dose of 50 mg·kg<sup>-1</sup> (Joubert, 1985). MT $\beta$  is weakly active at

all muscarinic receptor subtypes (Joubert, 1985; Jolkkonen *et al.*, 1995, 2001) and may thus interact with other molecular targets such as the adrenoceptors.  $\rho$ -Da1a is specific to the  $\alpha_{1A}$ -adrenoceptor (Quinton *et al.*, 2010). The third group, with 54 to 55% identity, contains MT2, MTLP-2 and MT7. MT7 is the only highly specific toxin for the M<sub>1</sub>-muscarinic receptor subtype (Servent and Fruchart-Gaillard, 2009), whereas MTLP-2 is not active at this receptor. The only other snake toxin described with adrenergic activity is  $\beta$ -cardiotoxin, which antagonizes  $\beta_1$ - and  $\beta_2$ -adrenoceptors at micromolar concentrations (Rajagopalan *et al.*, 2007). However, this toxin displays only 35% sequence identity with  $\rho$ -Da1b. Some toxins acting on muscarinic receptors have a higher sequence identity with  $\rho$ -Da1b than those acting on adrenoceptors. This suggests a relationship between these two pharmacological profiles with a potential cross-reactivity of three-finger-fold toxins for muscarinic receptors and adrenoceptors receptor families, as previously shown for the MT1 toxin (Harvey *et al.*, 2002). A detailed analysis of the few residues which interact these toxins with their respective targets initially requires a characterization of their precise pharmacological effects on the various subtypes of muscarinic receptors and adrenoceptors.

Very little is known about the molecular interactions between these toxins and their receptor targets, except for MT7, which exploits the tip of its three fingers (Fruchart-Gaillard *et al.*, 2008) to strongly interact with the second external loop of the M<sub>1</sub> muscarinic acetylcholine receptor (Kukkonen *et al.*, 2004). In the last decade, few structures of class A GPCRs have been solved (Palczewski *et al.*, 2000; Cherezov *et al.*, 2007; Rasmussen *et al.*, 2007; Jaakola *et al.*, 2008). If structural similarities

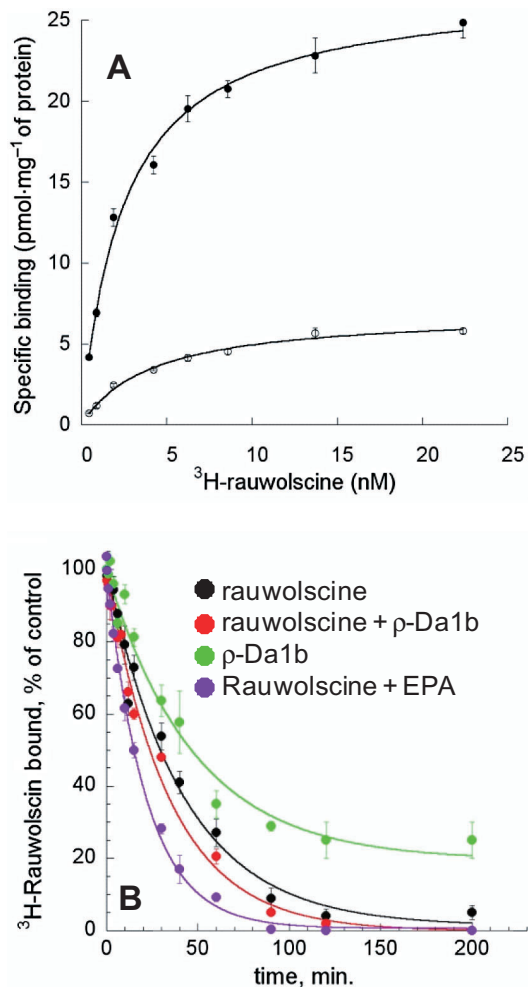


**Figure 7**

Characterization of the mode of action of  $\rho$ -Da1b on  $\alpha_{2A}$ -adrenoceptor expressed on CHO cells. (A) Saturation binding experiment of  $^3\text{H-rauwolscine}$  in the absence (●) or presence of  $\rho$ -Da1b (○, 10  $\mu\text{M}$ ). (B) Dissociation kinetic rate of  $^3\text{H-rauwolscin}$  bound, % of control in the presence of rauwolscine (black), rauwolscine plus  $\rho$ -Da1b (red),  $\rho$ -Da1b (green) and rauwolscine + 5-(N-ethyl-N-isopropyl)-amiloride (EPA) (purple).

between GPCRs reside mainly in their transmembrane domains, it is not the case for their external loops that are highly diverse in sequence and spatial organization (Palczewski *et al.*, 2000; Cherezov *et al.*, 2007; Rasmussen *et al.*, 2007; Jaakola *et al.*, 2008). Assuming that all three-finger-fold toxins interact with the external part of their molecular targets (as MT7 does), the structural organization of the external domains of each GPCR should account for the selectivity of the interacting toxin.

$\rho$ -Da1b interacts with  $\alpha_{2A}$ -adrenoceptors with an affinity of 14 nM for the  $\alpha_{2A}$ -adrenoceptor, showing a weak selectivity, five and three times, for  $\alpha_{2B}$ - and  $\alpha_{2C}$ -adrenoceptors, respectively. It is the first peptide ligand found to be specific for this receptor subfam-

ily, showing almost no activity at the other adrenoceptors.  $\rho$ -Da1b did not fully displace rauwolscine binding, leaving the same level of residual binding on each of the three  $\alpha_{2}$ -subtypes. To further investigate this residual binding, we performed  $^3\text{H-rauwolscine}$  saturation binding experiments in the presence of an excess of the toxin. Rauwolscine was still able to bind to the  $\alpha_{2A}$ -adrenoceptor with high affinity in these experiments, but the total number of sites available for binding was reduced by a factor of four. That rauwolscine could still bind receptors saturated with  $\rho$ -Da1b and with similar affinity suggests that two populations of receptor are present. Approximately 75% of the total receptor population is sensitive to  $\rho$ -Da1b; the remaining 25% is thus resistant to the toxin. We also examined the effect of  $\rho$ -Da1b on the dissociation rate of rauwolscine. We did not find a significant effect of the toxin, ruling out a potential allosteric mode of interaction. Additionally,  $\rho$ -Da1b added alone resulted in rauwolscine dissociation at the same rate as observed upon addition of yohimbine, confirming the competitive mode of action of the toxin. Moreover, only 80% of its binding was reversible, consistent with our findings from equilibrium binding experiments. Similar results had been previously obtained for  $\rho$ -Da1a, which does not fully inhibit  $^3\text{H-prazosin}$  binding on  $\alpha_{1A}$ -adrenoceptor and does not affect  $^3\text{H-prazosin}$  dissociation rate, suggesting a competitive mode of interaction of  $\rho$ -Da1a (Quinton *et al.*, 2010). By contrast, the MT7 toxin, which leaves residual binding at the  $M_1$  muscarinic receptor, substantially reduces the dissociation rate for  $^3\text{H-N-methyl-scopolamine}$  and was described as a potent negative allosteric modulator (Olianas *et al.*, 2000; Mourier *et al.*, 2003).

We used two different strategies for the functional characterization of the  $\rho$ -Da1b interaction. The first strategy involved monitoring conformational changes of the trimeric G protein induced upon receptor activation. We monitored this conformational rearrangement between G protein subunits by measuring BRET signal between a donor, the  $G\alpha$ -RLuc and an acceptor, the  $G\gamma$ -GFP (Gales *et al.*, 2006). This strategy allowed us to evaluate the effects of  $\rho$ -Da1b on one of the initial events in activation, leading to the characterization of this peptide toxin as an antagonist. The  $\alpha_{2A}$ -adrenoceptor is normally coupled to the  $G_i$  and  $G_s$  proteins and plays a role in a number of physiological functions. This receptor has been implicated in several disorders of the CNS [epilepsy, depression (Bekker and Sturaitis, 2005)] and others expressed in the periphery, such as diabetes, intestinal motility, cardiac function and pain (Rosengren *et al.*, 2009). We shifted its natural activation pathway to one

Table 2

Alignment of sequences for  $\rho$ -Da1b and various other toxins acting on adrenoceptors and muscarinic receptors

Edman's degradation Mass sequencing		LTXVTKDTIFGITTQNKPAQQLXCFIRRHYNHRYTEITRGXTATXPKPTNVRE----- -----ETIHCNTDKCNE			
Loops		-----1-----	-----2-----	-----3-----	%
$\rho$ -Da1b	Da	LTCVTKDTIFGITTQNKPAQQLXCFIRRHYNHRYTEITRGXTATXPKPTNVRETIHCNTDKCNE			
MT- $\alpha$	Dpp	LTCVTSKSIIFGITTENC PDGQNLFCFKWYILNHRYSDITWGCAATCPKPTNVRETIHCCETDKCNE			77
MT3	Da	LTCVTKNTIFGITTENC PDGQNLFCFKRWYIVIPRYTEITRGCAATCPIPENY-DSIHCCETDKCNE			76
MT4	Da	LTCVTSKSIIFGITTENC PDGQNLFCFKWYIVIPRYSDITWGCAATCPKPTNVRETIHCCETDKCNE			76
MT1	Da	LTCVTSKSIIFGITTENC PDGQNLFCFKWYIVIPRYSDITWGCAATCPKPTNVRETIHCCETDKCNE			74
MT- $\beta$	Dpp	LTCVTSKSIIFGITTEDCPDGQNLFCFKRRHYVVPKIYDITRGCVATCPIPENY-DSIHCCETDKCNE			67
$\rho$ -Da1a	Da	LTCVTSKSIIFGITTEDCPDGQNLFCFKRRHYVVPKIYDSTRGCAATCPIPENY-DSIHCCETDKCNE			66
Cm3	Dpp	LTCVTSKSIIFGITTEDCPDGQNLFCFKRRHYVVPKIYDITRGCVATCPIPENY-DSIHCCETEKCNN			64
MT2	Da	LTCVTSKSIIGVTTEDCPAGQNVCFKRWYVTPKNIYDIKGCATCPKVDNN-DPIRCGGTDKCN			55
MT7	Da	LTCVKSNSIWFPTSEDCPPGQNLFCFKRWYISPRMYDFTRGCAATCPKAEYR-DVINCCGTDKCNK			54
$\beta$ -ca	Oh	RKCLNTPLPLIYTT--CPIGQDKCVKMTIKKLP SKYDVIRGCDICPKSSA-DVEVLCCDTNKCNE			36

Percentage identity, relative to  $\rho$ -Da1b, is indicated for each sequence. Residues that differ from  $\rho$ -Da1b are in bold. Da, *Dendroaspis angusticeps*; Dpp, *Dendroaspis polylepis polylepis*; Nak, *Naja kaouthia*;  $\beta$ -Ca,  $\beta$ -cardiotoxin; Oh, *Ophiophagus hannah*.

mediated by a chimeric G protein, Gq-Top (Selvam *et al.*, 2010). This allowed  $\alpha_{2A}$ -adrenoceptor activation to be detected and quantified through measurement of calcium release. Yohimbine and  $\rho$ -Da1a induced rightward shifts of the activation curves without changing adrenaline efficacy. Schild regressions were clearly linear with a slope that deviated from unity for  $\rho$ -Da1b, suggesting that this ligand does not employ a simple competitive mode of action. The  $pA_2$  values for yohimbine determined using this system (5.93) were significantly lower than values found in the literature: 6.88 in the pineal gland (Pratt and Takahashi, 1987), 7.25 in the uterine artery (Ribeiro and Macedo, 1986) or 8.4 in the mesenteric artery (Agrawal *et al.*, 1984). This disparity could be due to the use of a chimeric G protein to funnel GPCR signal transduction to a common pathway involving  $Ca^{2+}$  release from intracellular stores. Indeed, shifts in agonist potency and efficacy have previously been shown, for example, upon co-transfection of receptors with  $G\alpha_{16}$  or with other chimeric G proteins (Kostenis, 2001). Our system may therefore have underestimated the potency of both yohimbine and  $\rho$ -Da1b, with  $pA_2$  values differing substantially from the affinity constants determined in binding experiments.

Further experiments are needed to check whether  $\rho$ -Da1b has similar pharmacological properties on the two other subtypes of  $\alpha_2$ -adrenoceptor and to determine the origin of the residual binding and non-competitive antagonist properties observed in our competition experiments. Studies are also needed, particularly at the molecular level,

to determine more precisely the interaction of  $\rho$ -Da1b with  $\alpha_2$ -adrenoceptors.

Nevertheless, the high affinity and selectivity of  $\rho$ -Da1b for this receptor subfamily make it a useful tool in the study of  $\alpha_2$ -adrenoceptors physiology and in the development of novel drug candidates. Thus, no  $\alpha_2$ -adrenoceptors antagonist are currently used clinically, although these receptors are involved in several pathologies such as intestinal motility (Blandizzi, 2007), orthostatic hypotension (Pang, 2001) or Parkinson's disease (Brotchie, 2005). This is largely because none of the compounds so far tested are sufficiently selective for  $\alpha_2$ -adrenoceptors (Crassous *et al.*, 2007). By itself,  $\rho$ -Da1b has no activity on any other adrenoceptor families. In addition, the natural venom fraction H, from which  $\rho$ -Da1b was isolated, shows no activity on 20 different GPCRs (N. Gilles, unpubl. data), suggesting that the  $\rho$ -Da1b selectivity covers a large number of aminergic GPCR. Finally, the peptide nature of the toxin should not allow it to pass the blood brain barrier, avoiding central side effects. For these reasons,  $\rho$ -Da1b has been patented and is under evaluation for treatments of several peripheral diseases.

## Acknowledgements

This work was supported by the French National Research Agency (L'Agence Nationale de la Recherche), as part of the programs adrenergicpeptides and gpcrcanotox.

We would like to thank Amelie Goudet for technical assistance and Jean-Philippe Pin (IGF, Montpellier, France) for the generous gift of the GqTop plasmid expression.

## Conflicts of interest

None.

## References

- Adem A, Asblom A, Johansson G, Mbugua PM, Karlsson E (1988). Toxins from the venom of the green mamba *Dendroaspis angusticeps* that inhibit the binding of quinuclidinyl benzilate to muscarinic acetylcholine receptors. *Biochim Biophys Acta* 968: 340–345.
- Agrawal DK, Triggle CR, Daniel EE (1984). Pharmacological characterization of the postsynaptic alpha adrenoceptors in vascular smooth muscle from canine and rat mesenteric vascular beds. *J Pharmacol Exp Ther* 229: 831–838.
- Alexander SP, Mathie A, Peters JA (2009). Guide to Receptors and Channels (GRAC). 4th edn. *Br J Pharmacol* 158 (Suppl. 1): S1–S254.
- Antosova Z, Mackova M, Kral V, Macek T (2009). Therapeutic application of peptides and proteins: parenteral forever? *Trends Biotechnol* 27: 628–635.
- Banerjee Y, Mizuguchi J, Iwanaga S, Kini RM (2005). Hemextin AB complex, a unique anticoagulant protein complex from *Hemachatus haemachatus* (African Ringhals cobra) venom that inhibits clot initiation and factor VIIa activity. *J Biol Chem* 280: 42601–42611.
- Becker S, Terlau H (2008). Toxins from cone snails: properties, applications and biotechnological production. *Appl Microbiol Biotechnol* 79: 1–9.
- Bekker A, Sturaitis MK (2005). Dexmedetomidine for neurological surgery. *Neurosurgery* 57: 1–10; discussion 1–10.
- Blandizzi C (2007). Enteric alpha-2 adrenoceptors: pathophysiological implications in functional and inflammatory bowel disorders. *Neurochem Int* 51: 282–288.
- Brotchie JM (2005). Nondopaminergic mechanisms in levodopa-induced dyskinesia. *Mov Disord* 20: 919–931.
- Carsi JM, Valentine HH, Potter LT (1999). m2-toxin: a selective ligand for M2 muscarinic receptors. *Mol Pharmacol* 56: 933–937.
- Changeux JP, Kasai M, Lee CY (1970). Use of a snake venom toxin to characterize the cholinergic receptor protein. *Proc Natl Acad Sci U S A* 67: 1241–1247.
- Chen Z, Rogge G, Hague C, Alewood D, Colless B, Lewis RJ *et al.* (2004). Subtype-selective noncompetitive or competitive inhibition of human alpha1-adrenergic receptors by rho-TIA. *J Biol Chem* 279: 35326–35333.
- Cheng Y, Prusoff WH (1973). Relationship between the inhibition constant (K1) and the concentration of inhibitor which causes 50 per cent inhibition (I50) of an enzymatic reaction. *Biochem Pharmacol* 22: 3099–3108.
- Cherezov V, Rosenbaum DM, Hanson MA, Rasmussen SG, Thian FS, Kobilka TS *et al.* (2007). High-resolution crystal structure of an engineered human 2-adrenergic G protein coupled receptor. *Science* 318: 1258–1265.
- Craig AG, Norberg T, Griffin D, Hoeger C, Akhtar M, Schmidt K *et al.* (1999). Contulakin-G, an O-glycosylated invertebrate neurotensin. *J Biol Chem* 274: 13752–13759.
- Crassous PA, Denis C, Paris H, Senard JM (2007). Interest of alpha2-adrenergic agonists and antagonists in clinical practice: background, facts and perspectives. *Curr Top Med Chem* 7: 187–194.
- Cruz LJ, de Santos V, Zafaralla GC, Ramilo CA, Zeikus R, Gray WR *et al.* (1987). Invertebrate vasopressin/oxytocin homologs. Characterization of peptides from *Conus geographus* and *Conus straitus* venoms. *J Biol Chem* 262: 15821–15824.
- Ducancel F (2005). Endothelin-like peptides. *Cell Mol Life Sci* 62: 2828–2839.
- Favreau P, Gilles N, Lamthanh H, Bournaud R, Shimahara T, Bouet F *et al.* (2001). A new omega-conotoxin that targets N-type voltage-sensitive calcium channels with unusual specificity. *Biochemistry* 40: 14567–14575.
- Fruchart-Gaillard C, Mourier G, Marquer C, Menez A, Servent D (2006). Identification of various allosteric interaction sites on M1 muscarinic receptor using 125I-Met35-oxidized muscarinic toxin 7. *Mol Pharmacol* 69: 1641–1651.
- Fruchart-Gaillard C, Mourier G, Marquer C, Stura E, Birdsall NJ, Servent D (2008). Different interactions between MT7 toxin and the human muscarinic M1 receptor in its free and N-methylscopolamine-occupied states. *Mol Pharmacol* 74: 1554–1563.
- Gales C, Van Durm JJ, Schaak S, Pontier S, Percherancier Y, Audet M *et al.* (2006). Probing the activation-promoted structural rearrangements in preassembled receptor-G protein complexes. *Nat Struct Mol Biol* 13: 778–786.
- Halai R, Craik DJ (2009). Conotoxins: natural product drug leads. *Nat Prod Rep* 26: 526–536.
- Han TS, Teichert RW, Olivera BM, Bulaj G (2008). Conus venoms – a rich source of peptide-based therapeutics. *Curr Pharm Des* 14: 2462–2479.
- Harvey AL, Kornisiuk E, Bradley KN, Cervenansky C, Duran R, Adrover M *et al.* (2002). Effects of muscarinic toxins MT1 and MT2 from green mamba on different muscarinic cholinergic receptors. *Neurochem Res* 27: 1543–1554.



- Jaakola VP, Griffith MT, Hanson MA, Cherezov V, Chien EY, Lane JR *et al.* (2008). The 2.6 angstrom crystal structure of a human A2A adenosine receptor bound to an antagonist. *Science* 322: 1211–1217.
- Jolkkonen M, Adem A, Hellman U, Wernstedt C, Karlsson E (1995). A snake toxin against muscarinic acetylcholine receptors: amino acid sequence, subtype specificity and effect on guinea-pig ileum. *Toxicon* 33: 399–410.
- Jolkkonen M, Oras A, Toomela T, Karlsson E, Jarv J, Akerman KE (2001). Kinetic evidence for different mechanisms of interaction of black mamba toxins MT alpha and MT beta with muscarinic receptors. *Toxicon* 39: 377–382.
- Joubert FJ (1985). The amino acid sequence of protein CM-3 from *Dendroaspis polylepis polylepis* (black mamba) venom. *Int J Biochem* 17: 695–699.
- King GF, Gentz MC, Escoubas P, Nicholson GM (2008). A rational nomenclature for naming peptide toxins from spiders and other venomous animals. *Toxicon* 52: 264–276.
- Kostenis E (2001). Is Galpha16 the optimal tool for fishing ligands of orphan G-protein-coupled receptors? *Trends Pharmacol Sci* 22: 560–564.
- Kukkonen A, Perakyla M, Akerman KE, Nasman J (2004). Muscarinic toxin 7 selectivity is dictated by extracellular receptor loops. *J Biol Chem* 279: 50923–50929.
- Kumar TK, Jayaraman G, Lee CS, Arunkumar AI, Sivaraman T, Samuel D *et al.* (1997). Snake venom cardiotoxins-structure, dynamics, function and folding. *J Biomol Struct Dyn* 15: 431–463.
- Leppik RA, Mynett A, Lazareno S, Birdsall NJ (2000). Allosteric interactions between the antagonist prazosin and amiloride analogs at the human alpha(1A)-adrenergic receptor. *Mol Pharmacol* 57: 436–445.
- McIntosh JM, Olivera BM, Cruz LJ (1999). Conus peptides as probes for ion channels. *Methods Enzymol* 294: 605–624.
- Mourier G, Dutertre S, Fruchart-Gaillard C, Menez A, Servent D (2003). Chemical synthesis of MT1 and MT7 muscarinic toxins: critical role of Arg-34 in their interaction with M1 muscarinic receptor. *Mol Pharmacol* 63: 26–35.
- Olianas MC, Maullu C, Adem A, Mulugeta E, Karlsson E, Onali P (2000). Inhibition of acetylcholine muscarinic M(1) receptor function by the M(1)-selective ligand muscarinic toxin 7 (MT-7). *Br J Pharmacol* 131: 447–452.
- Palczewski K, Kumasaka T, Hori T, Behnke CA, Motoshima H, Fox BA *et al.* (2000). Crystal structure of rhodopsin: a G protein-coupled receptor. *Science* 289: 739–745.
- Pang CC (2001). Autonomic control of the venous system in health and disease: effects of drugs. *Pharmacol Ther* 90: 179–230.
- Pratt BL, Takahashi JS (1987). Alpha-2 adrenergic regulation of melatonin release in chick pineal cell cultures. *J Neurosci* 7: 3665–3674.
- Putnam NH, Srivastava M, Hellsten U, Dirks B, Chapman J, Salamov A *et al.* (2007). Sea anemone genome reveals ancestral eumetazoan gene repertoire and genomic organization. *Science* 317: 86–94.
- Quinton L, Demeure K, Dobson R, Gilles N, Gabelica V, De Pauw E (2007). New method for characterizing highly disulfide-bridged peptides in complex mixtures: application to toxin identification from crude venoms. *J Proteome Res* 6: 3216–3223.
- Quinton L, Girard E, Maiga A, Rekik M, Lluell P, Masuyer G *et al.* (2010). Isolation and pharmacological characterization of AdTx1, a natural peptide displaying specific insurmountable antagonism of the alpha(1A)-adrenoceptor. *Br J Pharmacol* 159: 316–325.
- Rajagopalan N, Pung YF, Zhu YZ, Wong PT, Kumar PP, Kini RM (2007). Beta-cardiotoxin: a new three-finger toxin from *Ophiophagus hannah* (king cobra) venom with beta-blocker activity. *FASEB J* 21: 3685–3695.
- Rasmussen SG, Choi HJ, Rosenbaum DM, Kobilka TS, Thian FS, Edwards PC *et al.* (2007). Crystal structure of the human beta2 adrenergic G-protein-coupled receptor. *Nature* 450: 383–387.
- Ribeiro CA, Macedo TA (1986). Pharmacological characterization of the postsynaptic alpha-adrenoceptors in human uterine artery. *J Pharm Pharmacol* 38: 600–605.
- Rosengren AH, Jokubka R, Tojjar D, Granhall C, Hansson O, Li DQ *et al.* (2009). Overexpression of alpha2A-adrenergic receptors contributes to type 2 diabetes. *Science* 327: 217–220.
- Selvam C, Oueslati N, Lemasson IA, Brabet I, Rigault D, Courtiol T *et al.* (2010). A virtual screening hit reveals new possibilities for developing group III metabotropic glutamate receptor agonists. *J Med Chem* 53: 2797–2813.
- Servent D, Fruchart-Gaillard C (2009). Muscarinic toxins: tools for the study of the pharmacological and functional properties of muscarinic receptors. *J Neurochem* 109: 1193–1202.
- Servent D, Menez A (2001). Snake neurotoxins that interact with nicotinic acetylcholine receptors. In: Massaro EJ (ed.). *Handbook of Neurotoxicology*. Humana Press: Totowa, NJ, pp. 385–425.
- Servent D, Winckler-Dietrich V, Hu HY, Kessler P, Drevet P, Bertrand D *et al.* (1997). Only snake curaremimetic toxins with a fifth disulfide bond have high affinity for the neuronal alpha7 nicotinic receptor. *J Biol Chem* 272: 24279–24286.
- Sharpe IA, Gehrmann J, Loughnan ML, Thomas L, Adams DA, Atkins A *et al.* (2001). Two new classes of conopeptides inhibit the alpha1-adrenoceptor and noradrenaline transporter. *Nat Neurosci* 4: 902–907.

Suckau D, Resemann A, Schuerenberg M, Hufnagel P, Franzen J, Holle A (2003). A novel MALDI LIFT-TOF/TOF mass spectrometer for proteomics. *Anal Bioanal Chem* 376: 952–965.

Terlau H, Olivera BM (2004). Conus venoms: a rich source of novel ion channel-targeted peptides. *Physiol Rev* 84: 41–68.

Tytgat J, Chandy KG, Garcia ML, Gutman GA, Martin-Eauclaire MF, van der Walt JJ *et al.* (1999). A unified nomenclature for short-chain peptides isolated from scorpion venoms: alpha-KTx molecular subfamilies. *Trends Pharmacol Sci* 20: 444–447.

de Weille JR, Schweitz H, Maes P, Tartar A, Lazdunski M (1991). Calciseptine, a peptide isolated from black

mamba venom, is a specific blocker of the L-type calcium channel. *Proc Natl Acad Sci U S A* 88: 2437–2440.

Williams JA, Day M, Heavner JE (2008). Ziconotide: an update and review. *Expert Opin Pharmacother* 9: 1575–1583.

Wu PL, Lee SC, Chuang CC, Mori S, Akakura N, Wu WG *et al.* (2006). Non-cytotoxic cobra cardiotoxin A5 binds to alpha(v)beta3 integrin and inhibits bone resorption. Identification of cardiotoxins as non-RGD integrin-binding proteins of the Ly-6 family. *J Biol Chem* 281: 7937–7945.